Channel shortening and Viterbi algorithm based equalization for high data rate baseband communication over a frequency-selective channel

Paul Miqueu, Fabrice Belvèze, Jean-Marc Brossier, Laurent Ros

▶ **To cite this version:**

Paul Miqueu, Fabrice Belvèze, Jean-Marc Brossier, Laurent Ros. Channel shortening and Viterbi algorithm based equalization for high data rate baseband communication over a frequency-selective channel. Advances in Networks, Security and Communications, Vol. 4, book chapter "Channel shortening and Viterbi algorithm based equalization for high data rate base band communication over a frequency selective channel"., IFSA Publisinng, 2026, Advances in Networks, Security and Communications, Vol. 4, 978-84-09-47239-0. ⟨hal-05426603⟩

HAL Id: hal-05426603

https://hal.science/hal-05426603v1

Submitted on 19 Dec 2025

HAL is a multi-disciplinary open access archive for the deposit and dissemination of scientific research documents, whether they are published or not. The documents may come from teaching and research institutions in France or abroad, or from public or private research centers.

L'archive ouverte pluridisciplinaire **HAL**, est destinée au dépôt et à la diffusion de documents scientifiques de niveau recherche, publiés ou non, émanant des établissements d'enseignement et de recherche français ou étrangers, des laboratoires publics ou privés.

HAL Authorization

Channel shortening and Viterbi algorithm based equalization for high data rate baseband communication over a frequency-selective channel.

Miqueu Paul [12], Fabrice Belvèze[2], Jean-Marc Brossier[1], Laurent Ros[1]

Abstract

Considering a high data rate baseband communication serial link, we introduce three different receivers based on the Viterbi algorithm. The first one, named Falconer-MLSE, combines a channel-shortening linear filter proposed by Falconer and Magee and the Maximum Likelihood Sequence Estimator (MLSE) based on the Viterbi algorithm. The receiver's complexity is kept low but it remains very sensitive to thermal noise power. The second one, named DFE-MLSE, combines a partial Decision Feedback Equalizer (DFE) and the MLSE. It is supposed to amplify the thermal noise less than the linear filter but it is subject to error propagation. Also, the space occupied by the feedback loop on chip has to be tightly controlled, limiting the number of taps the linear filter in the feedback loop has. The third and last receiver introduced, named MLDFE, combines DFE and MLSE to limit the error propagation phenomenon. It is more complex than the DFE-MLSE but performs better in general. We then compare the performance of these receivers for a typical SerDes channel for optimal parameters before taking into account the requisites set by the IEEE standard working group and discriminating these receivers. We conclude that the best receivers under the standard constraints are the Falconer-MLSE receiver for a 4^{th} order Pulse Amplitude Modulation and the Falconer-DFE-MLSE, combination of a Falconer filter, a DFE and a Viterbi algorithm, for a 8^{th} order Pulse Amplitude Modulation and higher.

Keywords: SerDes link, Equalization, Channel shortening, Viterbi algorithm.

Table of acronyms

AWGN: Additive White Gaussian Noise
BER: Bit Error Rate
DFE: Decision Feedback Equalizer
FFF: FeedForward Filter
FBF: FeedBack Filter

[1]Gipsa-lab, Université Grenoble Alpes, CNRS, Saint Martin d'Hères, 38400
[2]STMicroelectronics, Grenoble 38000

IR: Impulse Response
MSE: Mean Square Error
MLSE: Maximum Likelihood Sequence Estimator
TIR: Target Impulse Response
VA: Viterbi Algorithm

Table of Contents

1.Introduction

When the frequency response of a channel is very different from that of the perfect (distortion-free) channel, transverse filtering may only be able to equalize the channel very imperfectly in a practical implementation. The transverse filter may need to have a very large number of coefficients, and it may also amplify noise significantly, resulting in high Bit Error Rate (BER) despite the elimination of Inter-Symbol Interference (ISI). It is in this context that nonlinear equalization solutions prove very useful for better symbol detection.

In 1979, C.A. Belfiore presented a history of non-linear equalization methods in [1] and concluded that the Maximum Likelihood Sequence Estimator (MLSE) offers the best compromise between performance, complexity, and implementation difficulty. This equalizer, based in practice on the Viterbi Algorithm (VA), initially proposed for convolutional code decoding [2][3], was proposed simultaneously by Forney [4], Omura [5] and Kobayashi [6]. In a much more recent publication focused on SerDes technology, the article [7] presents a very comprehensive state of the art of nonlinear equalization adapted to very high-speed serial links. Part of the state of the art combines Decision Feedback Equalization (DFE) and VA.

In the rest of this work, the VA will therefore be at the center of our receiver equalization strategy. This choice is corroborated by the state of the art, where more and more of the latest communication systems integrate VA at receiver. The second section introduces this MLSE block, detailing its operation and main characteristics.

As the computational complexity of the algorithm is critical, we then focus from section 3 to 6 on channel shortening upstream of VA by studying, in this context, state-of-the-art linear pre-filtering techniques and non-linear equalization techniques.

Finally, we compare in section 7, for each of the channel shortening methods presented, the performance of the communication system for a real-life frequency selective channel proposed by Richard Mellitz in [8] during a IEEE 802.3df working group meeting. This working group aims at establishing a standard for all communication systems using the Ethernet protocol for high data rates (above 100 Gbps).

This comparison part reports on our contributions in the field of nonlinear equalization of very high-speed serial links. An interpretation of the performance of each receiver is proposed, taking into account the advantages and disadvantages inherent in each equalization block. We conclude in section 8, in light of the specifications given by the standard, on the equalization method best suited to very high-speed serial links.

This chapter is an extension of the paper entitled “Miqueu, P., Belveze, F., Brossier, J. M., & Ros, L. (2025, February). Non-linear equalization techniques for high data rates serial links.” presented at the ARCI’2025 international conference, Automation, Robotics & Communications for Industry 4.0/5.0, p. 154.

2. The Maximum Likelihood Sequence Estimator (MLSE) using the Viterbi algorithm

Before Forney proposed in [4], concurrently with Omura and Kobayashi in [5], [6] and [9], to reuse the VA [2][3], initially designed for convolutional code decoding, in the context of equalization, the most naive method of sequence detection was to calculate the likelihood of all possible symbol sequences based on observations. As the complexity increased exponentially with the size of the symbol sequence considered, sequence detection in the sense of maximum likelihood was abandoned. MLSE, based on the VA, offers an optimal solution to the problem of estimating a sequence of symbols for a finite global channel impulse response with

complexity independent of the size of the sequence of symbols to be estimated. It evolves according to the size of the global channel impulse response at the input of the MLSE block.
Readers interested in understanding the reasoning behind the development of this algorithm and the details of its computations can refer to Forney's pioneering article [4], in which the VA is used for the first time to equalize a channel. Here, we only introduce the algorithm's features relevant when considering high data rate serial link equalization.

2.1 The Viterbi algorithm applied to equalization

The block scheme of the communication system we consider in this chapter is illustrated figure 1.

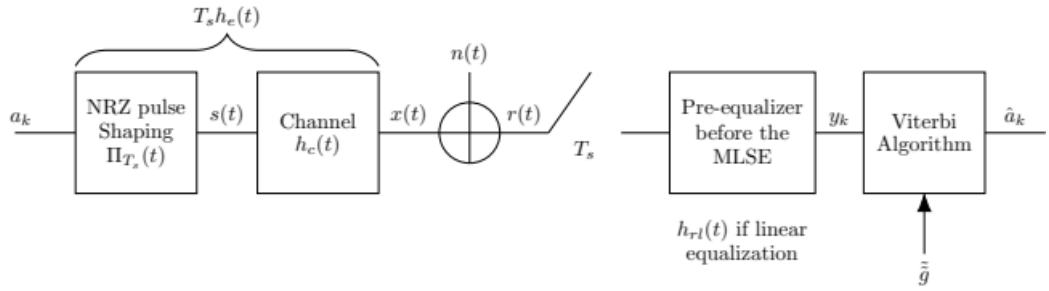

Figure 1 Block scheme of the communication system with a MLSE at the receiver

The analog received signal is $r(t) = T_s.\sum a_k h_e(t - kT_s)$ where a_k are the M-ary PAM symbols, h_e is the transmit impulse response, including rectangular symbol pulseshape $\Pi_{T_s}(t)$(unit amplitude during one symbol duration T_s) convolved by the channel impulse response$h_c(t)$(i.e. $h_e = \Pi_{T_s} * h_c$) and $n(t)$ is AWG noise with single-sided power spectral density N_0.

The VA takes as a parameter the partially equalized impulse response of the global channel denoted by $\tilde{\tilde{g}}$. The impulse response of the global channel, in the case where all the blocks that make up the communication system in figure 1 are filters, can be expressed as a convolution product such as:

$$\tilde{\tilde{g}}(t) = [\frac{1}{T_s}\Pi_{T_s} * h_c * h_{rl}](t) \qquad (1)$$

where $h_{rl}(t)$ is the impulse response of the linear reception filter before the MLSE. If the signal processing before the MLSE is not linear, the overall channel cannot be expressed as a convolution product. In particular, in the case where pre-equalization is provided by a DFE, we will construct a pseudo impulse response, the construction of which will be detailed later in section 4.
To be complete on the expression of the impulse response of the global channel at the VA input, we will say that in the case where it is not of finite size, it is truncated while trying to conserve as much energy as possible. If the coefficients of the global channel impulse response are unknown or vary slowly during transmission (which is not the case considered here), algorithms can be used to obtain them and track small variations [10], [11].

The VA algorithm will use a discrete-time version of the overall channel:

$$\tilde{\tilde{g}}_k = T_s \tilde{\tilde{g}}(t)|_{t=(k_0+k)T_s} \quad (2)$$

where k_0 is the delay (expressed in number of symbols) for sampling.
Therefore, considering a pseudo impulse response $\tilde{\tilde{g}}$ with $\nu + 1$ coefficients at the VA input and a zero symbol propagation delay in the communication chain ($k_0 = 0$), the samples at the VA input can be expressed as:

$$y_k = \lambda a_k + ISI_k + b_k \quad (3)$$

Where $\lambda = \tilde{\tilde{g}}_0$ and the ISI term can be expressed as

$$ISI_k = \sum_{n=k-\nu}^{k} a_n \tilde{\tilde{g}}_{k-n} \quad (4)$$

Since the impulse response of the overall channel is finite, we call the finite sequence of symbols participating in the ISI term at time k the memory configuration of the channel.
The memory configuration changes, resulting from symbol transmission, form a sequence for which the Viterbi algorithm provides an estimate that maximizes the likelihood in presence of Additive White Gaussian Noise (AWGN) and for a frequency selective channel [12].
Now that the relevant VA features have been introduced, we rise the reader's attention on several key points that have to be considered for high data rate serial link equalization.

2.2 To be remembered in the following

Firstly, although less complex than an exhaustive search for the sequence that maximizes likelihood, VA remains computationally complex. This is its main drawback. If the channel impulse response has $\nu + 1$ coefficients and the transmission alphabet contains M different symbols, the complexity of the VA will be $M^{\nu+1}$. The complexity increases exponentially with the size of the channel impulse response, making the use of the VA alone unfeasible in many practical cases. The prospect of taking advantage of the optimal equalization algorithm has generated a wealth of literature on different ways to reduce its complexity.
Secondly, VA requires knowledge of the impulse response.
Thirdly, in order to make a reliable decision on a symbol, VA needs to process τ samples after the sample of interest. This is the number of transitions in the trellis on which we traceback the sequence of symbols that maximizes the likelihood. This is a parameter that allows the reliability of the estimated symbol to vary. The deeper the backtracking, the greater the probability that the paths have converged to a single common ancestor, which guarantees the optimality of the decision. The backtracking length τ depends on the size of the impulse response of the overall channel at the input of the algorithm, denoted $\nu + 1$. We take $\tau = 5\nu$.
In order to limit computational complexity, which is the main challenge when it comes to using the VA for equalization, we have chosen to focus on channel shortening.

3. Channel shortening using linear filtering

While we can obtain the expression of the transverse filter for an ISI elimination criterion, linear filtering upstream of the VA pre-processes the signal to optimize VA performance. In some of the literature, this pre-filter is a whitened matched filter that ensures the best Signal to Noise Ratio (SNR) and white thermal noise at its output, which minimizes the probability of error at

the VA output [4]. We thus first introduce a communication system with a whitened matched filter and consider it as a reference. In other literature, it is shown that colored noise at the VA input has little effect on the error probability [19]. We will thus next consider an other pre-filter that seeks to limit the algorithmic complexity of the VA by shortening the channel impulse response as reducing algorithmic complexity is critical when implementing the VA.

3.1 Whitened matched filter

Following Forney's pioneering article [4], many methods for shortening the channel impulse response have emerged, each with its own advantages and disadvantages. Most articles in the literature consider that the receiver is equipped with a whitened matched filter at its input, ensuring that the signal is a sufficient statistic for determining the symbols sent. It is demonstrated in [13] for many performance criteria such as BER, BER after ISI equalization, and SNR, that adding a whitened matched filter does not degrade performance. We thus consider this communication system as a reference and begin by considering a receiver equipped with an whitened matched filter at its input.
The block linear analog Rx filter followed by a sampler in Figure 2 can then be broken down into an analog filter matched to the overall channel, a synchronous sampler at symbol rate, a digital whitening filter for thermal noise, and a digital channel shortening filter, as illustrated in Figure 3.

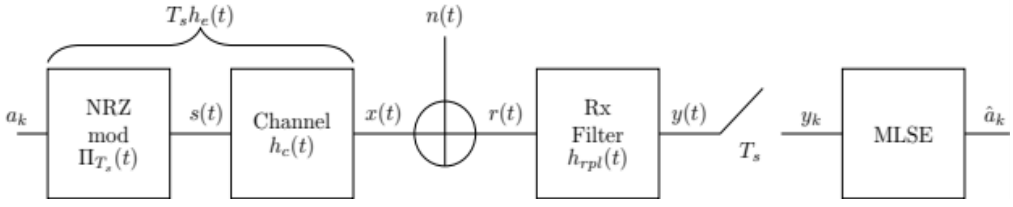

Figure *2* Communication system with a linear filter with impulse response h_{rpl} at Rx

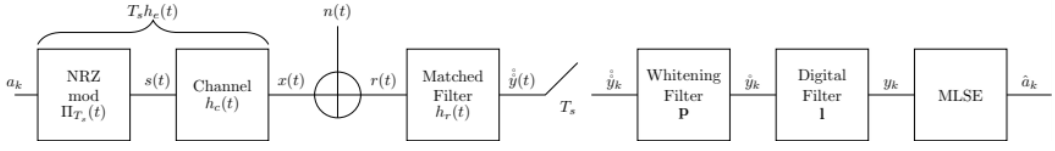

Figure *3* Communication system with linear filters corresponding to the linear filter with impulse response h_{rpl} at Rx illustrated in Figure *2*

Computation of the whithened matched filter is well known in the literature and we refer the reader to it for further details [4].
We only raise the reader's attention to the fact that, using the good computation criteria, the whitened matched filter can minimize the channel impulse response phase [4]. The impulse response of a minimum phase filter has remarkable properties, as it is the impulse response with maximum energy distribution over the first samples (which is very important, as we will see in section 4) and it is causally invertible.

We compare this reference communication system to another one, with a channel-shortening filter at the input of the MLSE, as it is supposed to reduce the computational complexity of the system at the price of a colored noise at the input of the MLSE.

3.2 Channel shortening using the Falconer and Magee's filter

The purpose of shortening the impulse response of the channel upstream of the VA is to transform it into a Target Impulse Response (TIR) that is shorter than the initial impulse response in order to reduce the complexity of the VA.

3.2.1 Foreword on channel shortening

Various studies exist on channel shortening. Qureshi and Hall proposed in [11] an adaptive receiver, based on the work of Lucky [15], that aimed at shortening the channel impulse response before the Viterbi algorithm and minimizing thermal noise power. The authors recommend obtaining the TIR by truncating the channel impulse response, which limits the Mean Square Error (MSE) at the equalizer output [16]. An analytical study of MLSE performance is conducted based on the size and coefficients of the TIR using the flow-graph technique proposed by Forney in [4]. Considering performance comparisons carried out in the literature [19], we decided to adopt a method proposed by Falconer and Magee in [17], which we introduce here.

3.2.2 Falconer and Magee filter principle

Falconer and Magee propose in [17] a transverse filter that takes as arguments the sampled impulse response of the overall channel and the number of TIR coefficients. This solution has the advantage of providing the impulse response of the channel-shortening filter at the same time as the TIR that will be used in the Viterbi algorithm. Under the constraint that the TIR energy is normalized, Falconer and Magee's algorithm, illustrated in Figure 4, minimizes the MSE between the output of the partial equalization filter for a given symbol sequence and the output of the TIR when fed with the given symbol sequence, while minimizing the thermal noise power. We refer the readers to [17] for computation details. The communication system with the channel shortening filter, noted as Falconer filter, is illustrated in Figure 5. The whitened matched filter is described as optional because we implement the receiver with and without this filter without modifying the algorithm for obtaining the Falconer filter coefficients. If the receiver does not have a matched filter at the input, the filter $h_{rp}(t)$ becomes the Kronecker delta function.

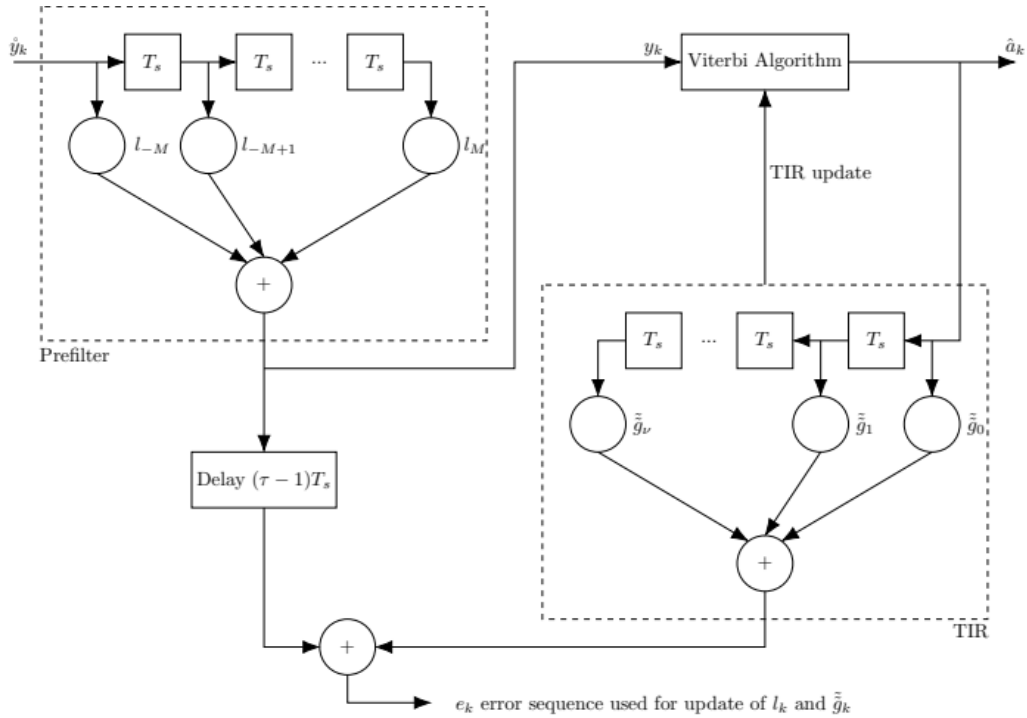

Figure 4 Receiver's structure proposed by Falconer and Magee.

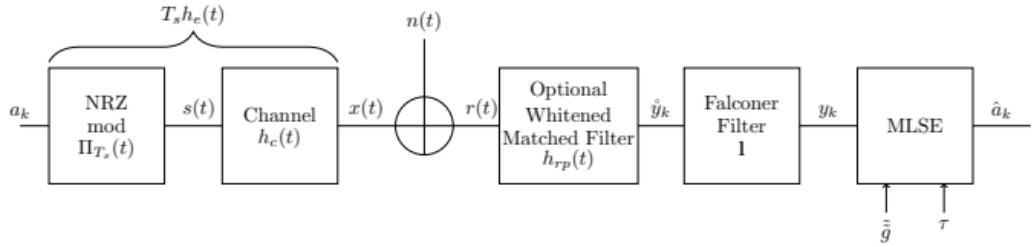

Figure *5* Communication system with a *digital* transverse filter proposed by Falconer and Magee in [17] which taps are arranged in the vector $\mathbf{l}$. Decision is taken by a MLSE. Its parameters are the TIR $\tilde{\tilde{g}}$ and the traceback depth τ of the VA.

Beare, in [19], notes that the VA is only optimal when the thermal noise at its input is white, a condition that is not met when using the method described in [11] or [17]. The author therefore proposes using the TIR whose spectrum is as close as possible to the spectrum of the original channel, given the limited size of the TIR. The author does not seek to minimize the power of the thermal noise at the output of the linear filter, and the experimental results he obtains do not show any improvement in performance for the scenario of interest. We will therefore stick with Falconer's filter.

As part of our research, we implemented the Falconer and Magee filter, with and without a whitened matched filter, for the channel proposed by Richard Mellitz during a session of the

IEEE 802.3df work group on the standard. Characteristics of various channels are available in [8]. We chose the 0.5 meter long backplane link with 1mm large SMA connectors and a PCB loss of 3.2dB which S-parameters can be found in the sma_1.0mm_3.2dB_500mm_NVAC_thru.s4p file.
S-parameters for the considered as well as for other channels (various lengths, connectors or PCB loss) are freely available at [39]. We compute, from the S-parameters, the channel's impulse response using the fft and an over-sampling ratio of 2^{10} and illustrate it in Figure 6.2. The spectrum directly given by the S-parameters is illustrated in Figure 6.1.

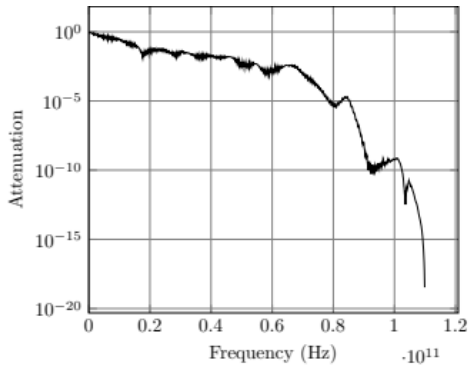

Figure *6*.1 Power spectral density of the channel proposed by Richard Mellitz in [8]

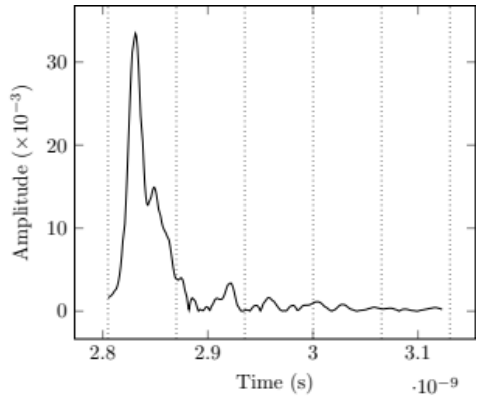

Figure *6*.2 Channel's I.R. The space inbetween two dotted lines corresponds to a 10 symbols period gap for a 4-PAM and a binary data rate of 224 Gbps.

Figure *6 Power spectral* density and impulse response (I.R.) of the channel proposed by Richard Mellitz. It corresponds to a backplane link of length 500mm linked to a chip by sma connectors of 1.0 mm diameter and a 3.2 dB attenuation on the chip.

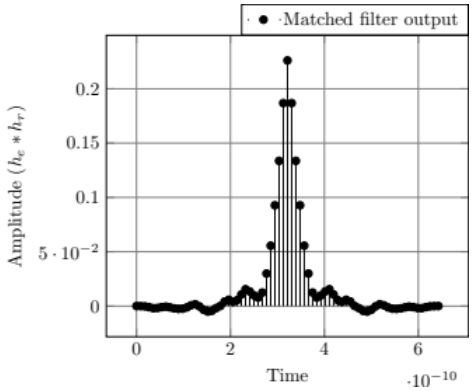

Figure *7*.1 Global channel I.R. at the matched filter output for a 4-PAM.

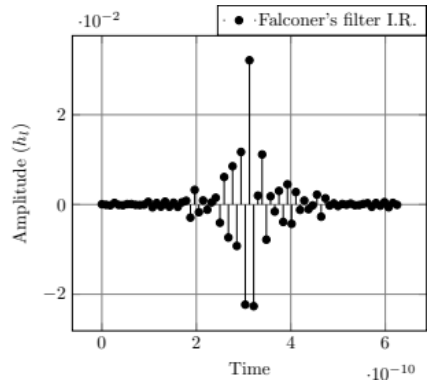

Figure *7*.2 Falconer's filter I.R. for $\nu + 1 = 4$, $N_{FM} = 71$ coefficients

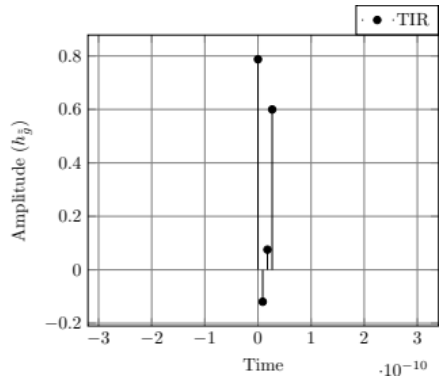

Figure *7*.3 TIR at the output of the Falconer's filter $\nu + 1 = 4$**,** $N_{FM} = 71$

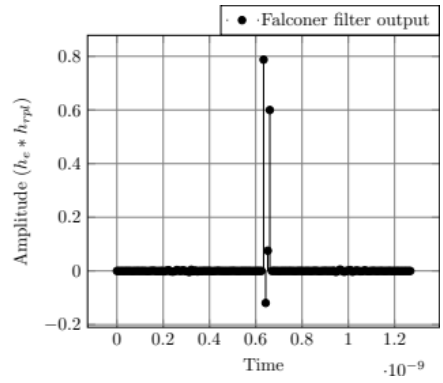

Figure *7*.4 Convolution between the global channel I.R. and the Falconer filter for $\nu + 1 = 4$**,** $N_{FM} = 71$ **coefficients**

Figure *7* Global channel at the output of the matched filter I.R.(*7.1*), Falconer's filter I.R. (*7.2*), TIR (*7.3*) and I.R. of the global channel at the output of the Falconer filter (*7.4*) for $\nu + 1 = 4$**,** $N_{FM} = 71$ **with a matched filter at Rx.**

Are illustrated Figure 7 for a 4-PAM, a TIR size of $\nu + 1 = 4$ coefficients, a Falconer filter of $N_{FM} = 2M + 1 = 71$ coefficients, and a receiver with a whitening filter at the input:

- The impulse response of the channel at the output of the matched filter alone $h_e * h_r(t)|_{t=kT_s}$,
- The impulse response of the Falconer filter $h_l(t))_{t=kT_s}$ for $N_{FM} = 71$ and $\nu + 1 = 4$ coefficients,
- The TIR $\tilde{g}(t))_{t=kT_s}$ for $N_{FM} = 71$ and $\nu + 1 = 4$ coefficients,
- The impulse response of the channel at the output of the Falconer filter $(h_{erp} * h_l)(t)|_{t=kT_s}$,

We note that the impulse response of the overall channel shown in 7.4, considering the coefficients containing most of the signal energy and neglecting a little ISI, corresponds to the TIR in 7.3. This filter is therefore a good candidate for channel shortening, reducing the overall channel IR from approximately 26 to approximately 4 non-zero coefficients for 4-PAM.
Similarly, when there is no matched filter at the receiver, Figures 8.1 and 8.2 illustrate the TIR and the impulse response of the overall channel with $\nu + 1 = 4$, $N_{FM} = 71$.

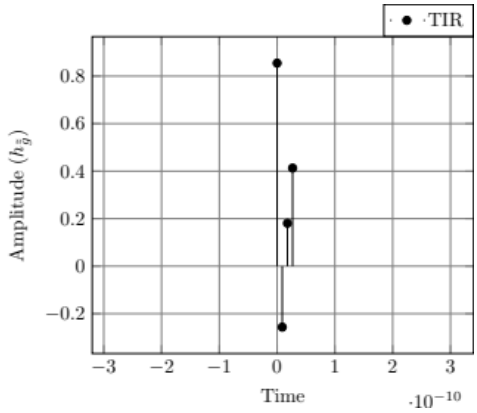

Figure *8*.1 TIR with $\nu + 1 = 4$, $N_{FM} = 71$.

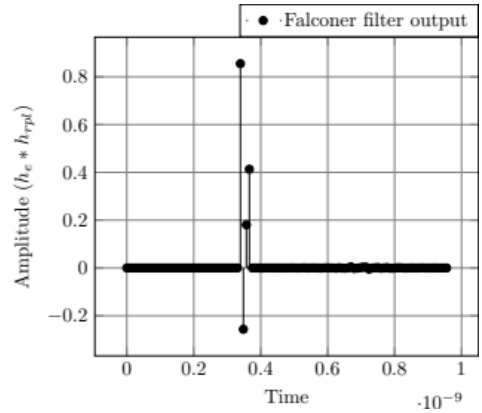

Figure *8*.2 Overall channel with $\nu + 1 = 4$, $N_{FM} = 71$.

Figure *8* TIR (a) and I.R. of the overall channel at the output of the Falconer's filter for $\nu + 1 = 4$, $N_{FM} = 71$ and without a matched filter at Rx.

As already mentioned earlier in this paper, thermal noise amplification is the main drawback of linear filtering. For performance comparison purpose, we thus turn to nonlinear equalization applied to channel shortening.

4. Channel shortening using Decision Feedback Equalizer (DFE)

The article by C.A. Belfiore [1] provides a very comprehensive overview of DFE. Initially presented as a suboptimal alternative to MLSE, DFE does indeed perform less well than MLSE, but its complexity varies linearly with the size of the overall channel impulse response. It also amplifies thermal noise less than a linear filter [20] but can be subject to error propagation. We first introduce the DFE as proposed in [21] and [22], which we refer to as the traditional DFE. Next, we explain how it can shorten, in the form of a partial DFE, the impulse response of the overall channel upstream of the MLSE, as proposed in [23].

4.1 Structure and principle of a traditional DFE

The classic structure of the receiver with DFE is illustrated in Figure 9.

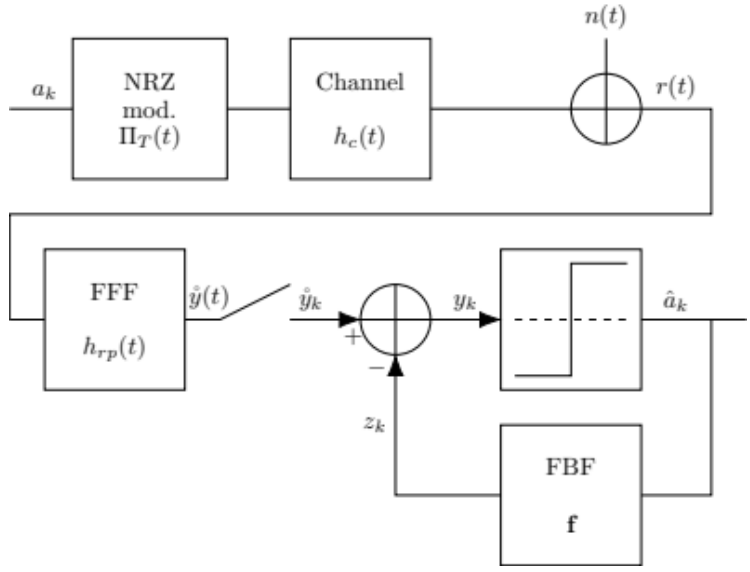

Figure 9 Traditional structure of a DFE at Rx with Feed-Forward Filter (FFF) and FeedBack Filter (FBF).

The signal at the output of the channel is first filtered by the Feed-Forward Filter (FFF)

$$\mathring{y}(t) = [r * h_{rp}](t)$$

The impulse response of the output of the FFF is denoted by $\tilde{g}$ (that means $\tilde{g} = h_e * h_{rp}$). At the output of the FFF, the signal is sampled, then a sum of decisions weighted by the coefficients of the FBF filter stored in the vector denoted by f is subtracted from it, as shown in Figure 9. The FBF filter hasN_{fbf}coefficients. We have:

$$f_n = \tilde{g}_{n+1} \text{for} n \in \{0, N_{fbf} - 1\}$$

We then have:

$$z_k = \sum_{n=0}^{N_{fbf-1}} f_n \hat{a}_{k-n+1} \qquad (5)$$

where $\hat{a}_k$ are the estimates, at the output of the decision block, of the symbols sent. The sum expressed in equation (4), known as the post-cursor ISI, aims to cancel out the ISI generated by the symbols preceding the symbol of interest by subtraction at the output of the FFF. We then have:

$$y_k = \mathring{y}_k - z_k$$

the signal samples on which the decision is made. The decision on the sample of interest y_k is then made by choosing the amplitude in the modulation dictionary that minimizes the MSE between the amplitude of z_k and the amplitudes in the modulation dictionary. The impulse response of the equivalent overall channel after subtraction of the post-cursor ISI is such that:

$$\tilde{\tilde{g}}_k = \begin{cases} \tilde{g}_0 for k = 0 \\ 0 otherwise \end{cases}$$

4.2 Calculation of FFF and FBF coefficients

In the following and throughout the literature, the decisions made are assumed correct when they are used to determine the coefficients of the optimal FFF and FBF filters, for example. In other words: $\hat{a}_k = a_k$. The coefficients of the FFF and FBF can be calculated adaptively [24]. Since the channel is assumed known here, we calculate the coefficients analytically. There are three criteria for determining the coefficients of the FFF and FBF:

- Zero Forcing criterion at the DFE output [25]
- Minimum Mean Squared Error criterion between the decision made and the sample before the decision [26]
- Minimum Error Probability criterion at the DFE output [27]

It is demonstrated in [20] that the ZF criterion and the MMSE criterion are equivalent for the considered scheme. Also, as we only plan to use the DFE to shorten the input channel of a VA the third criterion is not relevant in our case. We therefore calculate the DFE coefficients using the ZF criterion, which, according to [28], makes the FFF the whitened matched filter that minimizes the channel phase.

4.2.1 DFE with FFF whitened matched filter

Referring to the literature, we first implement the receiver with a whitened matched filter. The coefficients of the FFF and FBF, as well as the impulse response of the channel at different points of the DFE, are illustrated in Figure 10.

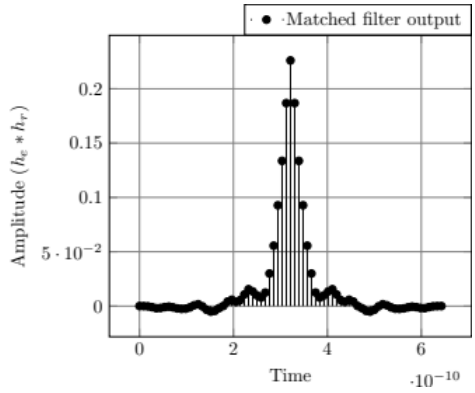

Figure 10.1 *M*atched filter output $h_e(\tau) * h_r$

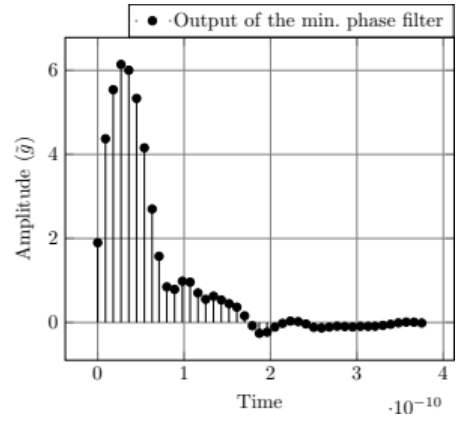

Figure 10.2 4-PAM minimum phase channel $\tilde{g}$

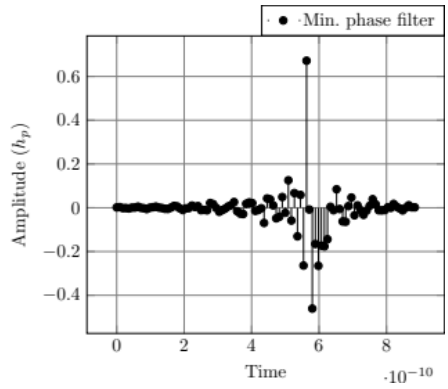

Figure 10.3 FFF h_p

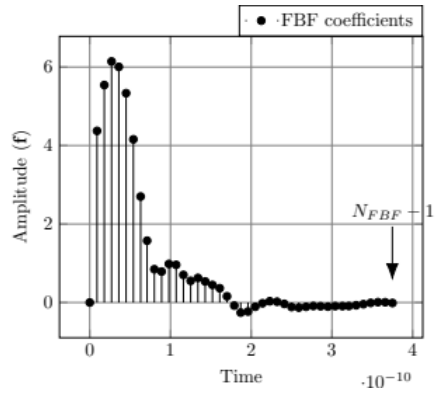

Figure 10.4 FBF f

F*igure 10* I.R. of the channel at the output of the whitened matched filter(*10.1*), of the minimum phase channel (*10.2*), of the FFF (*10.3*) and of the FBF (*10.4*) for a 4-PAM and considering the whitening matched FFF with $N_{FFF} = 100$.

The FFF, which impulse response is denoted h_{rp}, is decomposed into an analog filter adapted to the overall transmission channel, which impulse response is denoted h_r, and a digital whitened filter that corrects the phase of the impulse response h_p. The impulse response $\tilde{g}$ of the channel at the output of the phase-correcting whitening filter is minimum phase.
Under the ZF criterion, the coefficients of the FBF are equal to the coefficients of the impulse response of $\tilde{g}$ (channel at the output of the FFF) for complete elimination of the post-cursor ISI. We can see this by comparing Figure 10.2 and Figure 10.4, which differ only by the first coefficient.

4.2.2 DFE with FFF phase-correcting all-pass filter

For comparison purposes, we implement the receiver without a matched filter at the receiver. In this case, the FFF is the phase-correcting all-pass filter with impulse response h_p. Referring to Figure 9, we have $h_{rp} = h_p$. The output channel of the FFF is minimum phase but has the same frequency response as the input channel. Note that the impulse response of the FFF is a truncated version to which a delay, denoted δ_{FFF}, is added because the stable impulse response of the phase-correcting all-pass filter is infinite in duration and non-causal when g (the impulse response of the FFF input channel) is not already at minimum phase.
In the rest of this document, a receiver without a matched filter will have a phase-correcting all-pass filter.
The impulse responses of the FFF and the channel at different points in the receiver without a matched filter are illustrated in Figure 11 at the output of the Mellitz channel already introduced [8].

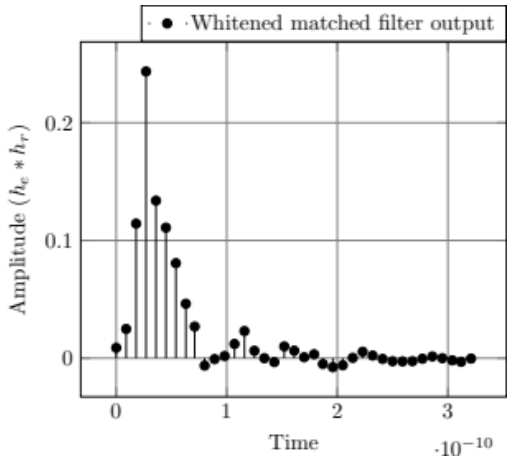

Figure 11.1 Whitened matched filter output $h_e(\tau) * h_r$

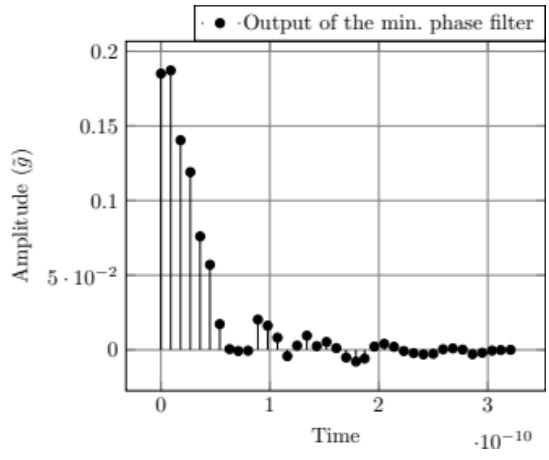

Figure 11.2 4-PAM minimum phase channel $\tilde{g}$

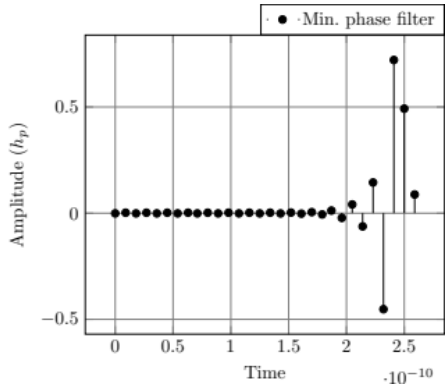

Figure 11.3 FFF h_p

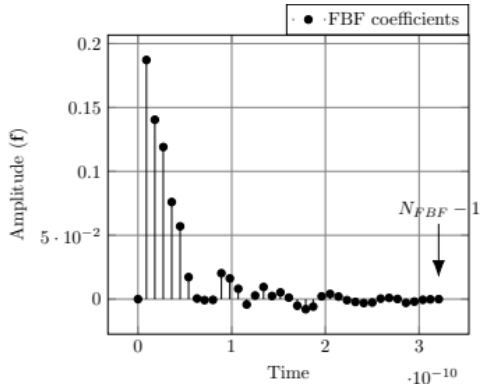

Figure 11.4 FBF f

Figure 11 *Global Tx channel (11.1), minimum phase channel (11.2), FFF (11.3) and FBF (11.4) for a 4-PAM and considering a FFF without a matched filter such that* $N_p = 30$.

4.2.3 Performance comparison

We compare, in Figure 12, the performance of the two communication systems.

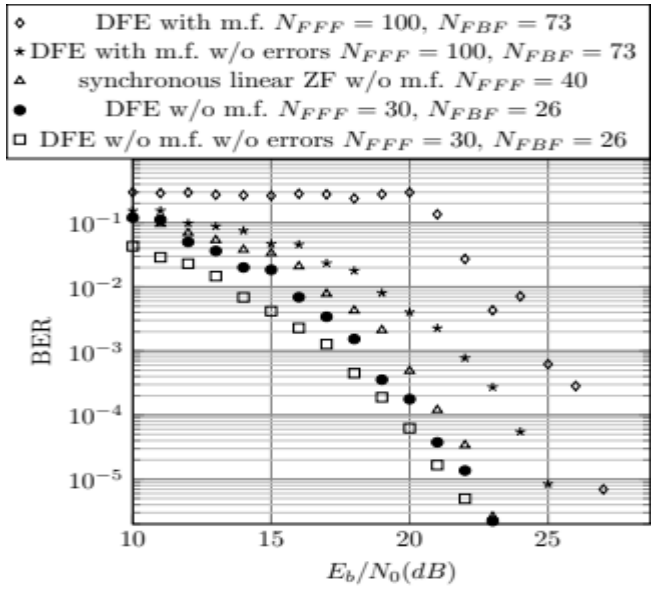

Figure 12 Performance comparison of the communication systems, with and without matched filter (m.f.), for a 4-PAM.

The number of coefficients in the FFF and FBF differs for the two systems considered because they depend on the shape and size of the impulse response of the overall channel at the DFE input. The FFF must have more coefficients when a matched filter is present in order to correctly minimize the channel phase. If the impulse response of the overall channel at the output of the FFF has $\nu + 1$ coefficients, the FBF has ν taps.

The performance of the "error-free" DFE, corresponding to the DFE without error, is plotted for comparison. The "error-free" DFE differs from the traditional DFE in the nature of the symbols at the input of the FBF. Whereas in the traditional DFE, the symbols at the input of the FBF are the decisions made by the DFE, in the "error-free" DFE, they are the symbols actually sent. The equation (4) becomes:

$$z_k = \sum_{n=0}^{N_{fbf}-1} f_n a_{k-n+1}$$

The performance of the "error-free" DFE can be simulated to provide a benchmark, but the system cannot be implemented in practice because the symbols sent are unknown to the receiver.

Finally, the performance of a synchronous linear ZF filter in the absence of the matched filter is also plotted to demonstrate the superiority of the DFE over linear filtering in this case [38].

We observe in Figure 12 the superiority of the receiver without a matched filter with an all-pass phase correction filter. The E_b/N_0 gap is approximately of 5 dB for a BER of 10^{-5} between the two DFE. We also note the impact of error propagation in the DFE in the presence of a matched filter. This very strong error propagation is due to the shape of the impulse response of the overall channel at the output of the FFF, illustrated in Figure 10.2, which is very different from the ideal strictly decreasing minimum phase impulse response. The impulse response shown in

Figure 11.2 for a receiver without a matched filter is closer to the ideal shape, which results in a small performance difference between a traditional DFE and an "error-free" DFE.
To demonstrate the need to obtain the minimum phase channel at the output of the FFF, we illustrate in Figure 13 the performance of the communication system when the impulse response at the input of the DFE is the impulse response of the overall channel at transmission, illustrated in Figure 11.1.

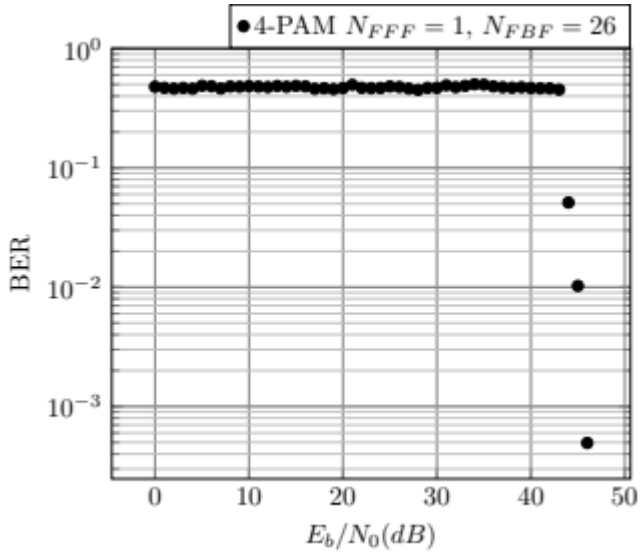

Figure *13* Communication system performance with a DFE without matched filter but with an all-pass phase correcting filter $N_{FFF} = 1$ and $N_{FBF} = 26$.

In this case, the impulse response of the FFF is the Kronecker delta function and the FBF is the digital impulse response of the overall transmission channel (except for the index coefficient 0). We can see in Figure 13 that the performance of the communication system only improves for values of E_b/N_0 greater than 41 dB. Below this, we observe the effects of very probable error propagation on performance.
When shortening the channel upstream of an MLSE block, only partial equalization is necessary, which allows us to use only reduced-amplitude FBF coefficients and thus reduce the magnitude of error propagation. The idea of shortening the channel upstream of an MLSE using a DFE was first presented in [23] and is now considered in certain equalization methods for very high-speed serial links [29].

4.3 Structure and principle of the partial DFE

To distinguish between DFE for channel shortening and DFE for channel equalization, which we have just introduced, we refer to the former as partial DFE, equipped with partial FBF whose impulse response is denoted by f', and the latter as complete DFE, equipped with complete FBF whose impulse response is denoted by f. We illustrate the partial DFE in Figure 14.

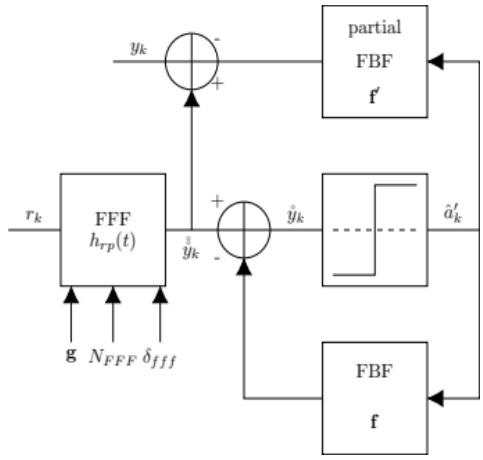

Figure *14* Block diagram of the partial DFE. The inputs to the partial FBF are the outputs of a conventional DFE (with a full FBF). The samples y_k are the transmitted symbols that have passed through the partially equalized channel. They are *the inputs of* the MLSE.

For a given channel, the FFF is the same for the full DFE as for the partial DFE. The vector f′ containing the coefficients of the impulse response of the partial FBF can be expressed in terms of the elements of the vector f containing the coefficients of the full FBF as:

$\mathrm{f}' = \{0, \ldots, 0, f_{\nu+1}, \ldots, f_{N_{FBF}-1}\}^T$

for a channel shortened to $\nu + 1$ coefficients and a full FBF with N_{FBF} coefficients.

We illustrate the coefficients of the partial FBF and the impulse response of the equivalent channel at the DFE output for the receiver with a matched filter in Figure 15 and Figure 16 for the receiver without a matched filter.

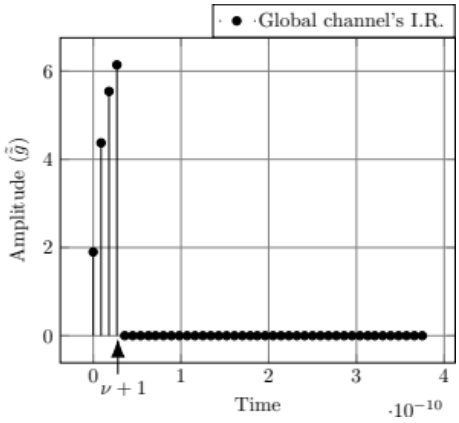

Figure *15*.1 Corresponding global channel I.R.

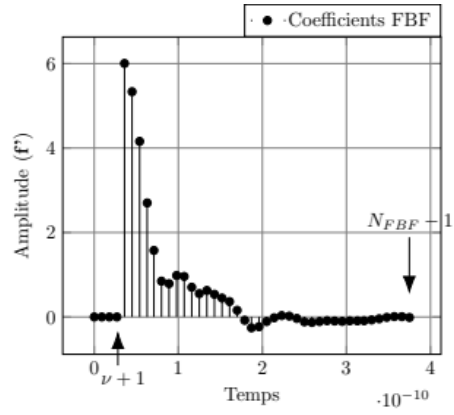

Figure *15*.2 Partial FBF coefficients

Figure *15* Impulse response of the corresponding global channel after partial DFE and partial FBF coefficients for a receiver with matched filter for a 4-PAM, $N_{FFF} = 100$, $N_{FBF} = 73$ and $\nu + 1 = 4$.

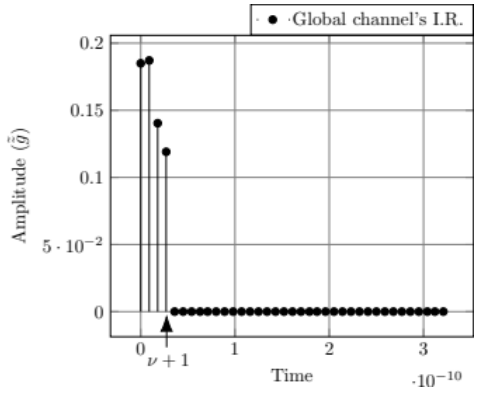

Figure *16*.1 Corresponding global channel I.R.

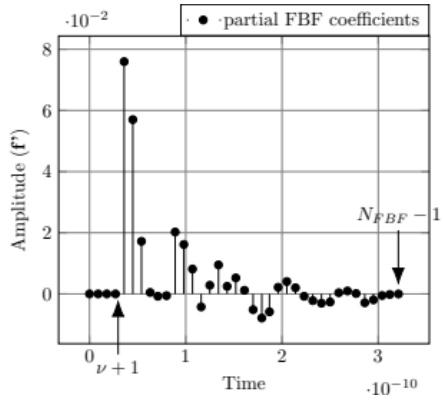

Figure *16*.2 Partial FBF coefficients

Figure *16* Impulse response of the corresponding global channel after partial DFE and partial FBF coefficients for a receiver without matched filter (replaced by a all-pass phase correcting filter) for a 4-PAM, $N_{FFF} = 30$, $N_{FBF} = 26$ and $\nu + 1 = 4$.

In both cases, since the partial FBF coefficients have smaller amplitudes and are fewer in number than the complete FBF coefficients, we can expect the error propagation due to the DFE feedback loop to be reduced compared to the complete DFE.
Below, we describe the equalization block combining MLSE and DFE for channel shortening and list its advantages and disadvantages.

5. Decision Feedback Equalization followed by a Maximum Likelihood Sequence Estimator – DFE-MLSE

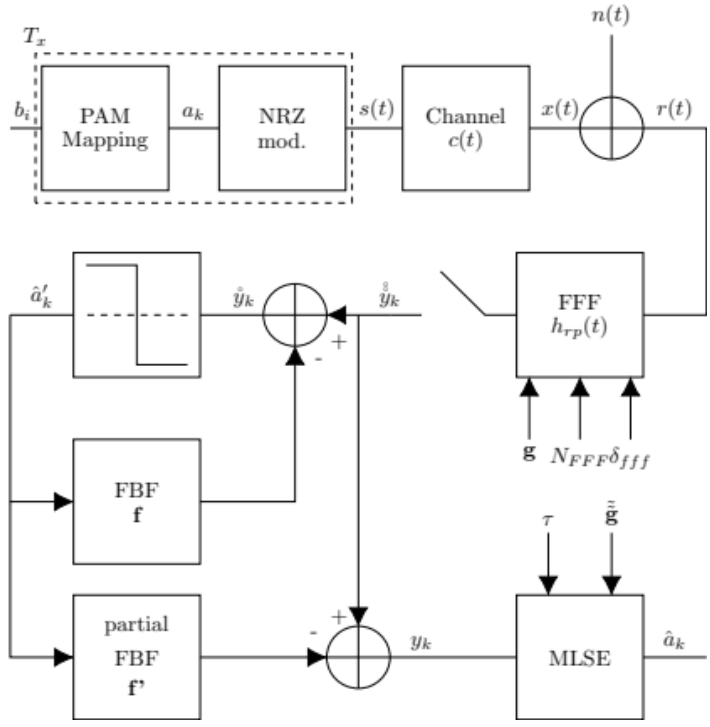

Figure *17* DFE-MLSE: Channel shortening using the partial FBF followed by the MLSE. Decisions at the input of the partial FBF are made by a conventional FBF.

The communication system studied is illustrated in Figure 17. We reuse the complete DFE and partial DFE that we introduced in the previous section. Thus, the FFF can be broken down into an analog prefilter matched to the overall transmission channel followed by a transverse filter, or it can consist exclusively of a transverse filter. Both cases are studied, and the impulse response with and without matched filter is illustrated in Figures 10 and 11, respectively, for a global channel impulse response at the MLSE input of size $\nu + 1 = 4$. The output signal of the FFF, denoted $\mathring{\mathring{y}}$, passes through a complete DFE on one side and a partial DFE on the other. The coefficients of the FBF of the complete DFE are stored in the vector $f = \{\tilde{\tilde{g}}_1, \tilde{\tilde{g}}_2, \ldots, \tilde{\tilde{g}}_{N_{FBF}}\}$ and the decision made by the complete DFE is denoted by $\hat{a}'_k$. We have:

$$\mathring{y}_k = \mathring{\mathring{y}}_k - \sum_{n=0}^{N_{FBF}-1} f_n \hat{a}'_{k-n-1}$$

The decisions $\hat{a}'_k$ then pass into the partial FBF, whose $N_{FBF'}$ coefficients are stored in f' before being subtracted from the signal $\mathring{\mathring{y}}$ at the output of the FFF to partially eliminate the ISI. We have:

$$\overset{\circ}{\overset{\circ}{y}}_k = \overset{\circ}{\overset{\circ}{y}}_k - \sum_{n=0}^{N_{FBF}-1} f'_n \hat{a}'_{k-(\nu+1)-n}$$

$$\overset{\circ}{\overset{\circ}{y}}_k = \overset{\circ}{\overset{\circ}{y}}_k - \sum_{n=\nu+1}^{N_{FBF}-1} f_n \hat{a}'_{k-n}$$

$$\overset{\circ}{\overset{\circ}{y}}_k = \overset{\circ}{\overset{\circ}{y}}_k - \sum_{n=\nu+1}^{N_{FBF}-1} \tilde{\tilde{g}}_{n-1} \hat{a}'_{k-n}$$

With $\nu + 1$ being the size of the partially equalized channel at the input of the MLSE block.
Finally, the partially equalized signal y enters the MLSE, whose state machine and weights associated with its transitions are functions of the TIR denoted by $\tilde{\tilde{g}}$ and the number of non-zero coefficients of the TIR denoted by $\nu + 1$.
The size $\nu + 1$ of the impulse response of the overall channel upstream of the MLSE is determined by computational complexity constraints. The VA makes reliable decisions on the partially equalized signal, reducing the probability of error compared to a simple DFE. Propagation error is limited because the accuracy of the ISI calculation is less decisive in the final decision. Thus, a decision error has less impact on the decision on subsequent symbols.

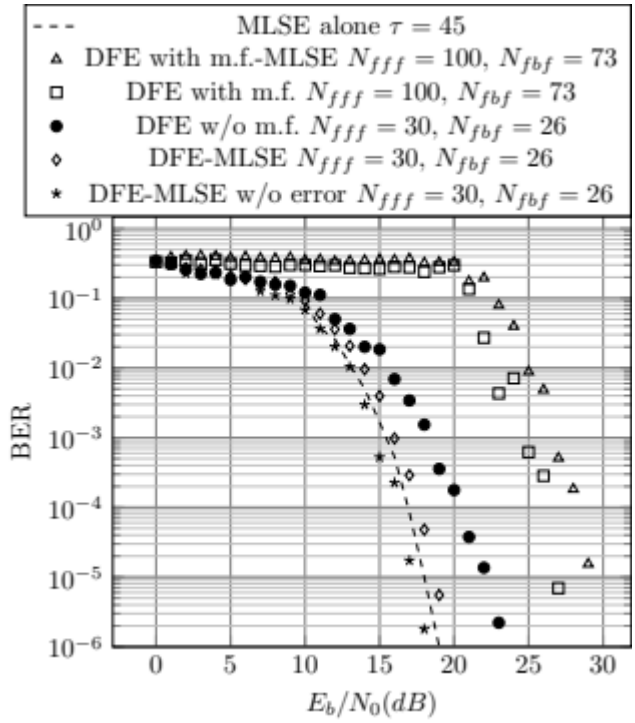

Figure *18* BER comparison of communication systems for a 4-PAM and $\nu + 1 = 4$. Performances of the MLSE alone are also plotted for $\nu + 1 = 10$

We observe in Figure 18 a performance gain of more than 3 dB for a BER of 10^{-5} enabled by the addition of an MLSE block at the output of the partial DFE for $\nu + 1 = 4$. When we compare this to Figure 12, we note that the DFE-MLSE receiver achieves better performance than the error-free DFE. Also, the difference between the conventional DFE-MLSE and the error-free

DFE-MLSE is less than 1 dB for a BER of approximately 10^{-5}, which is comparable, when looking at Figure 12, to the performance difference between the conventional DFE and the error-free DFE.

When there is a matched filter at the receiver input, performance is significantly degraded by error propagation, regardless of whether or not there is an MLSE block. Figure 10 clearly shows that the partial FBF coefficients are conducive to error propagation because they have amplitudes comparable to the amplitudes of the coefficients of $\tilde{\tilde{g}}$.

We plotted the performance of the VA alone, for a backtracking depth $\tau = 45$, without pre-filtering at the channel output, and observed that it is (very slightly) better than that of the DFE-MLSE. This observation was expected because the VA is the optimal receiver. To limit the duration of simulations, the impulse response that the VA considers at its input is reduced to $\nu + 1 = 10$ coefficients, compared to ≈ 40 coefficients for the complete impulse response illustrated in Figure 18, which reduces the performance of the VA. If we were not constrained by the execution time of the algorithm, we would observe that the performance of the VA alone is at least as good as the performance of the DFE-MLSE without error.

To place this study in the context of very high-speed serial links, we note that, with or without a matched filter, the impulse response of the overall channel at the output of the FFF filter has many non-zero coefficients. However, in the specific case of very high-speed serial links, feedback control is difficult to implement because the passage through the FBF must last less than the symbol period and the occupancy of the FBF on the chip must be minimal. According to the literature on the subject, these temporal and spatial constraints allow the DFE's FBF to have only one or two coefficients [30]. To circumvent this limitation, techniques such as sliding block DFE [31] and loop break DFE [32] have been proposed in the literature on very high-speed serial links, but are out of scope of this paper.

6. Combination of DFE and MLSE - MLDFE

Finally, the last receiver we consider is the MLDFE, because better performance can be achieved by using an MLSE at the output of a partial DFE, at the cost of greater complexity. Since the decision made by the VA is more reliable than the decision made by the DFE threshold function, Gu and Le Ngoc propose in [33] to feed the decisions made by the VA back into the DFE. The receiver is illustrated in Figure 19.

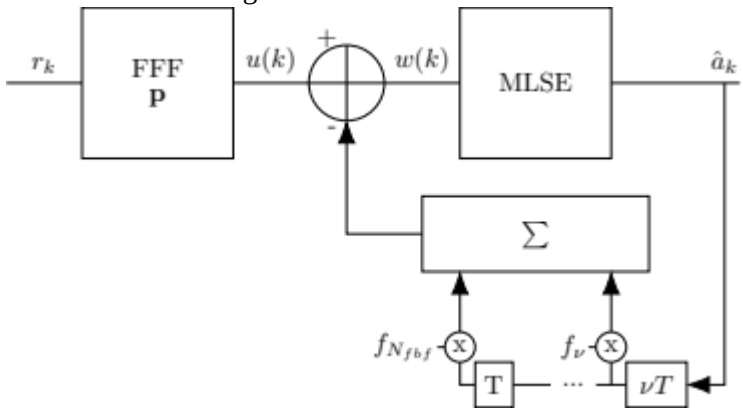

Figure *19* Combination between DFE and MLSE. Decision made by the MLSE is sent back to the input of the partial FBF.

We consider a sequence of L transmitted symbols and a MLSE tracking depth of τ states such that $L > \tau$.

In the case of the DFE-MLSE considered in the previous section, the MLSE processed a sequence of L samples after passing through the partial DFE and estimated a sequence of L symbols.

In this section, for the MLDFE, the MLSE processes a sequence of τ samples at each iteration, estimates a sequence of τ symbols, and delivers only the oldest symbol in this sequence as the final decision. The complete sequence of τ symbols is sent to the FBF to calculate the next τ samples. The sample sequences y_k at the MLSE input therefore overlap on $\tau - 1$ indices but are not necessarily identical because the VA has provided a new sequence estimate.

For each sequence of τ symbols entering the MLSE, the trellis is opened using a preamble consisting of the previous ν final decisions.

We translate this into equations. The sequence of τ samples at the MLSE input can be expressed as:

$\mathrm{y} = \mathrm{Ap} - \mathrm{Bf'}$

where y is a column vector of size $\tau \times 1$, A is a matrix $\tau \times N_{fff}$, **p** is a column vector $N_{fff} \times 1$ containing the FFF coefficients, B is a matrix $\tau \times [N_{fbf} - (\nu))$ and **f'** is the column vector $[N_{fbf} - \nu] \times 1$ containing the FBF coefficients. A contains the channel output observations:

$$\mathrm{A} = \begin{pmatrix} r_k & r_{k+1} & \cdots & r_{k+N_{fff}-1} \\ r_{k+1} & r_{k+2} & \cdots & r_{k+N_{fff}-2} \\ \cdots & \cdots & \cdots & \cdots \\ r_{k+\tau-1} & r_{k+\tau} & \cdots & r_{k+\tau+N_{fff}-1} \end{pmatrix}$$

The sequence estimated by the VA is denoted by $\mathrm{o} = \{\hat{a}_k, o_1, \cdots, o_{\tau-1}\}$ with $\hat{a}_k$ being the final decision and o_i being the other estimated symbols in the sequence. B is the matrix consisting of estimates denoted by o_i with $i \in [\![0, \tau - 1]\!]$ when they are temporary, and denoted by $\hat{a}_{k-i}$ with $i \in [\![1, N_{fbf}]\!]$, when the decision is final. Thus[3]:

$$\mathrm{B} = \begin{pmatrix} \hat{a}_{k-\nu} & \hat{a}_{k-\nu-1} & \cdots & \hat{a}_{k-N_{FBF}} \\ \hat{a}_{k-\nu+1} & \hat{a}_{k-\nu} & \cdots & \hat{a}_{k-N_{FBF}+1} \\ \cdots & \cdots & \cdots & \cdots \\ \hat{a}_k & \hat{a}_{k-1} & \cdots & \hat{a}_{k-N_{FBF}+\nu} \\ o_1 & \hat{a}_k & \cdots & \hat{a}_{k-N_{FBF}+\nu+1} \\ \cdots & \cdots & \cdots & \cdots \\ o_{\tau-1-\nu} & o_{\tau-\nu-2} & \cdots & o_{\tau-\nu-N_{FBF}} \end{pmatrix}$$

In the following section, we illustrate the performance of this receiver and compare it to the performance of other previously introduced receivers.

7. Performance comparison through simulation

As already mentioned above, the performance of a nonlinear equalizer is difficult to describe analytically. It is possible to frame the performance with bounds in the case of MLSE or to give an upper limit of performance by neglecting error propagation in the case of DFE, but to get a precise idea of the performance of communication systems equipped with different receivers, we must resort to simulations. We therefore propose to compare the performance of the different nonlinear equalization methods presented using simulations. We first compare the performance

[3] Note that $o_{\tau-\nu-N_{FBF}}$ may not exist depending on the system parameters. If $\tau > N_{FBF} + \nu$, it exists. Otherwise, this element is 0. Given the orders of magnitude of N_{FBF} relative to τ, this borderline case is anecdotal. Also, in matrix B, we note that the element in the upper left corner is not $\hat{a}_k$ because the partial DFE only shortens the channel.

of the receivers without constraining the complexity and then we compare the performance taking into account the limitations set by the standard.

7.1 Performance comparison without complexity constraints

We consider the channels, already presented above, proposed by R. Mellitz to the IEEE 802.3df working group [8]. The characteristics of these channels have already been illustrated in Figure 6. These characteristics are the result of experiments and physical models to determine the frequency attenuations due to passage through the substrate and impedance differences.
Given that, for finite filter sizes and the frequency-selective channels studied, the communication system with an matched filter performs less well than the communication system without an matched filter, in this section we are only interested in the communication system without an matched filter at the receiver. We also consider that the receiver is equipped with a filter that provides a minimum phase global channel at the input of the channel shortening pre-equalizer. The receiver of the communication system under consideration is illustrated in Figure 20 for the Falconer-MLSE and the DFE-MLSE. The "channel shortening pre-equalizer" block can either be a Falconer filter or a channel shortening DFE.

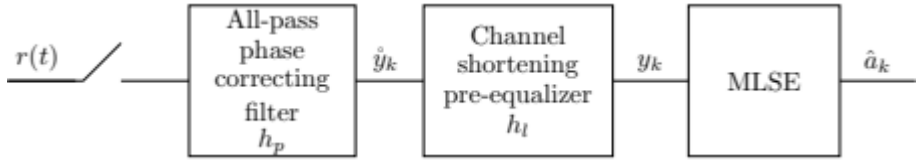

Figure *20* Receiver block schemme with channel shortening pre-equalizer.

The channel phase correction passband filter has $N_p = 10$ coefficients, the minimum size required to correctly render the phase of the channel considered minimal in 4-PAM.
For channel shortening using Falconer's linear filter, the number of coefficients that make up the filter is determined experimentally. We have determined that the performance of the Falconer-MLSE communication system is best for $N_{FM} = 71$.
In practice, the two digital filters can be combined to form a single filter.
The performance of the receivers is illustrated in Figure 21 for a partially equalized global channel impulse response of $\nu + 1 = 4$ coefficients and a 4-PAM, initially.

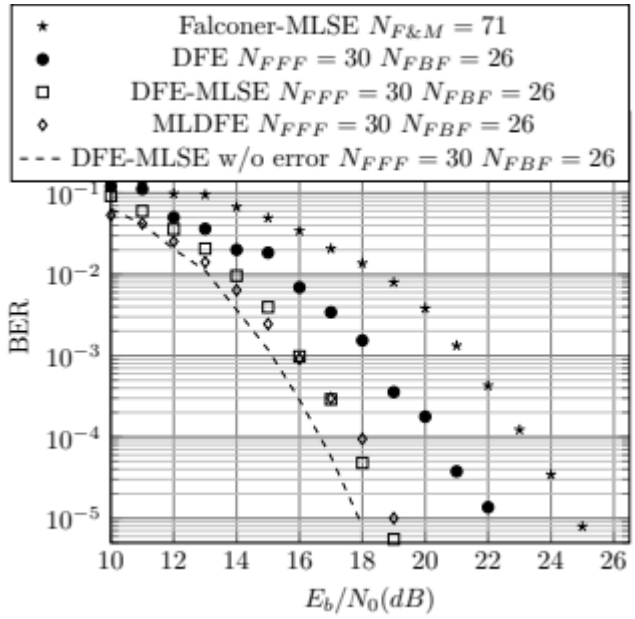

Figure *21* Performance comparison between non-linear equalization algorithms for the channel proposed by Mellitz, for a 4-PAM *and for* $\nu + 1 = 4$.

We are interested in performance differences between receivers for a BER of 10^{-5}. We observe that the method of channel shortening using the Falconer filter followed by MLSE is the least efficient communication system among those studied. The use of DFE alone provides a gain of 3 dB. Channel shortening using DFE followed by estimation using the Viterbi algorithm provides a gain of 3 dB compared to DFE alone. Finally, the performance gap between MLDFE and DFE-MLSE is less than 0.5 dB in favor of DFE-MLSE.

To assess the influence of the size of the impulse response of the MLSE input channel on the relative performance of the receivers, we perform the same simulations for $\nu + 1 = 5$. Greater computing power is allocated to MLSE.

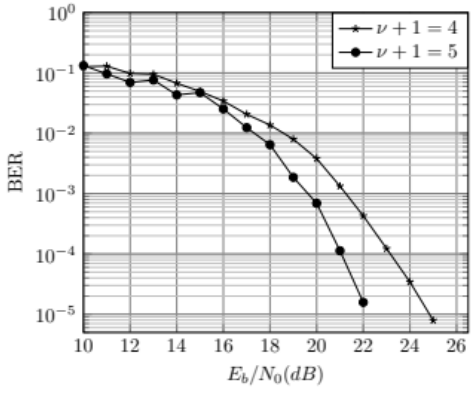

Falconer-MLSE $N_{FM} = 71$

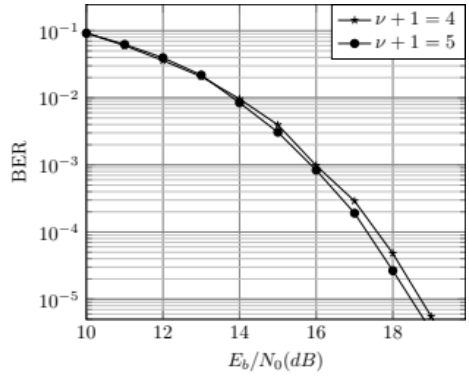

DFE-MLSE $N_{FFF} = 30, N_{FBF} = 26$

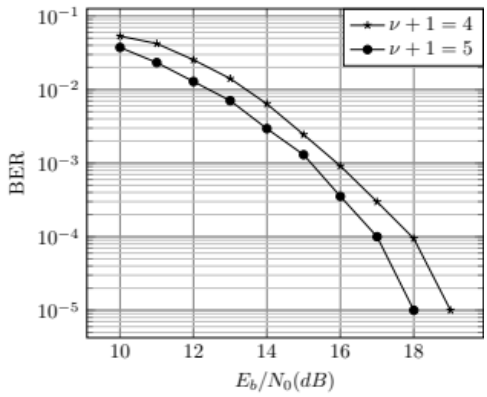

MLDFE $N_{FFF} = 30, N_{FBF} = 26$

Figure *22* Performance comparison between non-linear equalization algorithms for the channel proposed by Mellitz for $\nu + 1 = 4$ **et** $\nu + 1 = 5$**.**

Channel shortening using a transverse filter is always the least effective method. However, the performance gap between DFE alone and Falconer filter followed by MLSE is reduced to less than 2 dB for a BER of 10^{-5} after comparison with Figure 22. The performance of DFE followed by MLSE is significantly improved by 0.4 dB, and the performance of MLDFE (or MLDFE without error, not shown here) is improved by 1dB. MLDFE performs better than DFE-MLSE in this case.

This comparison shows the benefits of increasing the size of the shortened channel impulse response for Falconer-MLSE, DFE-MLSE, and MLDFE. However, computational complexity increases with the increase in the size of the impulse response of the partially equalized channel at the MLSE input. The complexity of the Viterbi algorithm is multiplied by 4 for a 4-PAM when ν increases by 1.

After illustrating the performance of receivers for 4-PAM in Figure 21, we illustrate their performance for 8-PAM in Figure 23 for a fixed bit rate.

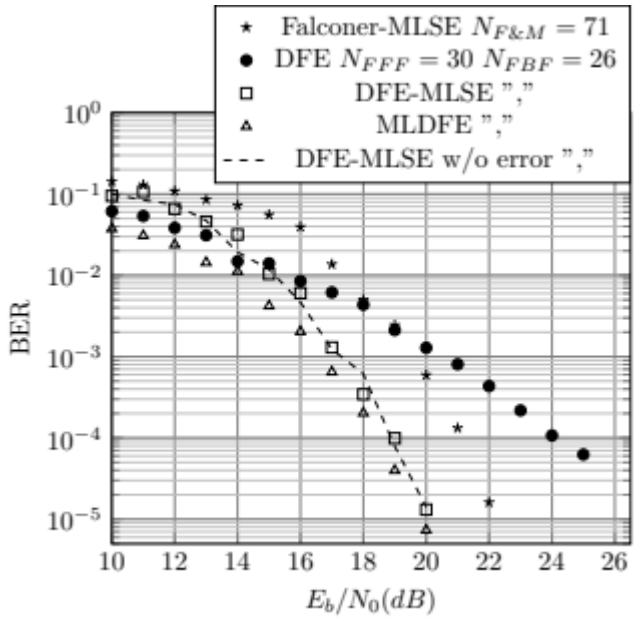

Figure *23* Performance comparison between different receivers for $\nu + 1 = 5$ *and for a* 8-PAM

We observe a deterioration in receiver performance involving decision feedback compared to 4-PAM. Only Falconer-MLSE performs identically to 4-PAM. DFE-MLSE corresponds to DFE-MLSE without error. We conclude that for $\nu + 1 = 5$, there is no error propagation in this receiver.

We note that in the case of SerDes links operating at 224 Gbps, the standard deviation of time jitter is of the order of $\sigma_j = 0.01T_b$. That means 1% of the bit period. We have verified that for such a low level of jitter, its effect is not noticeable on receiver performance. To observe the effect of jitter, its standard deviation would need to be 10 times higher, of the order of $\sigma_j = 0.1T_b$.

7.2 Performance comparison under standard constraints

Considering very high data rate serial links, a receiver is fit if it verifies some constraints. It has to reach a BER of 10^{-5}, or lower,for aE_b/N_0equal to 30 dB before decoding according to the standard [40]. The computational complexity has to be kept to its minimum, thus the impulse response of the overall channel at the MLSE input is reduced to $\nu + 1 = 2$, the minimum size for the Viterbi algorithm to perform better than a threshold decision block. Finally, because both occupied area on the chip has to be small and timing delay constraints when using a feedback loop are very tight, the FBF of the channel shortening DFE can only have up to two coefficients [30].

To verify the standard's constraints in terms of computational complexity and performance without coding, we propose a receiver with a Falconer filter, DFE, and MLSE in series, which performance for different parameters is illustrated in Figure 24.

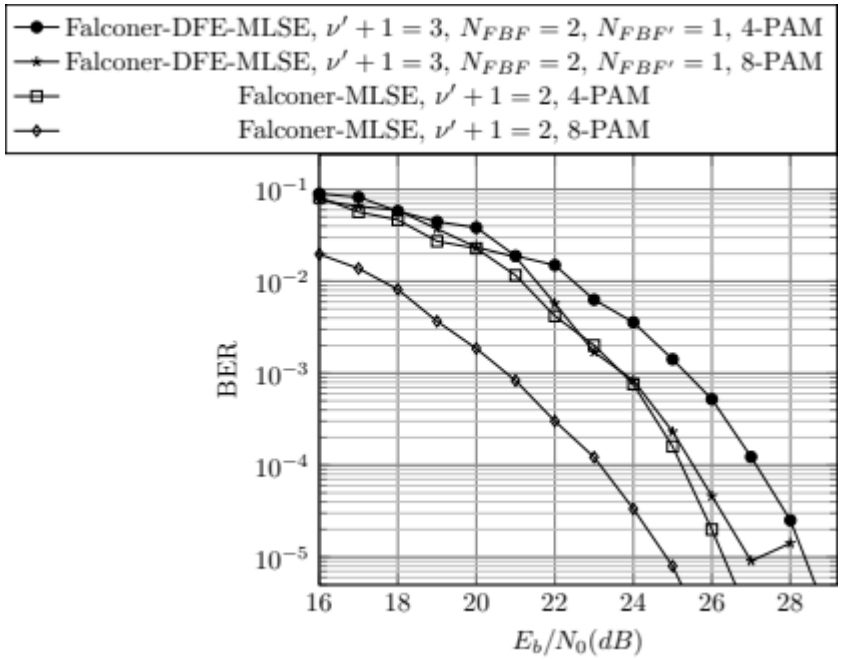

Figure *24* Performance comparison between *receivers* Falconer-DFE-MLSE with *all-pass phase correcting filter* $N_p = 10$**, *Falconer filter*** $N_{FM} = 71$**, DFE depending o*n* the use case** $N_{FFF} = 1$**,** $N_{FBF} = 2$**,** $N_{FBF'} = 1$ ***and*** **MLSE** $\nu + 1 = 2$**.**

We compare Figure 24, the performance of Falconer-DFE-MLSE with the performance of Falconer-MLSE for a 4-PAM and an 8-PAM. We denote $\nu' + 1$ as the size of the impulse response at the output of the Falconer filter and $\nu + 1$ as the size of the impulse response at the input of the VA. In the case of Falconer-MLSE, we have $\nu = \nu'$. In the case of Falconer-DFE-MLSE, since the full FBF can only have a maximum of two coefficients and $\nu + 1 = 2$, we have $\nu' + 1 = 3$ and therefore a partial FBF with $N_{FBF'} = 1$ coefficient.

For a 4-PAM, we observe that the performance of the Falconer-MLSE receiver is better than the performance of the Falconer-DFE-MLSE by 2 dB for a BER of 10^{-5}.

For 8-PAM, the performance of the Falconer-DFE-MLSE receiver reaches an error floor for an BER of 10^{-5} due to error propagation (as verified experimentally), while the Falconer-MLSE has no error floor.

When we allow the Falconer-DFE-MLSE's full FBF to have 3 coefficients, this receiver has a 2dB gain for a BER of 10^{-5} compared to the Falconer-MLSE, as shown in Figure 25.

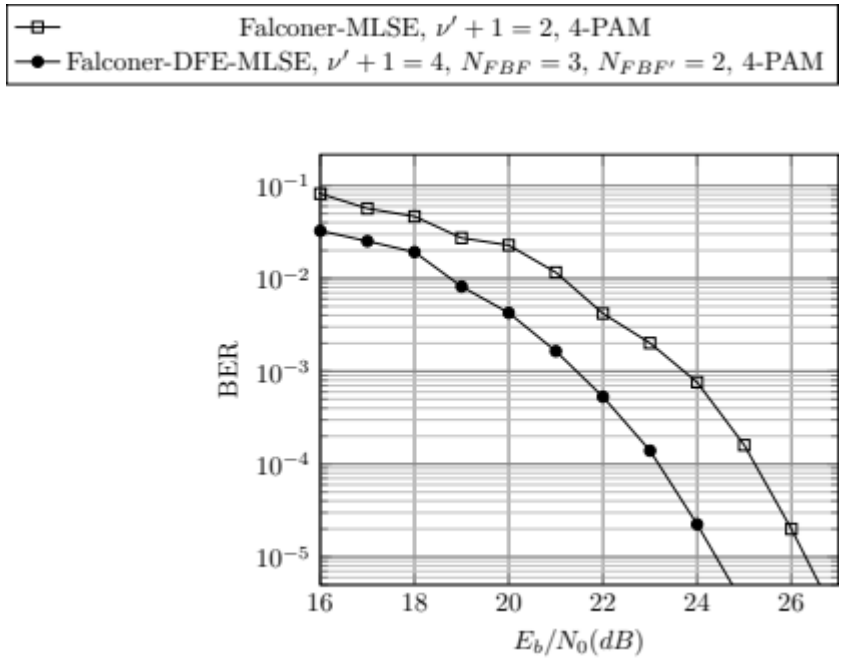

Figure *25* Performance comparison between Falconer-DFE-MLSE *with* $\nu' + 1 = 4$**,** $N_{FBF} = 3$**,** $N_{FBF'} = 2$ ***and*** **Falconer-MLSE**

We conclude that Falconer-DFE-MLSE remains interesting if we disregard the spatial occupancy constraint that limits the number of FBF coefficients.
Since the standard specifications require a BER of less than 10^{-5} for a $E_b/N_0 = 30dB$ ratio [40], we conclude that for a 4-PAM, the proposed Falconer-DFE-MLSE receiver meets the specifications for limited computational complexity and a FBF coefficient number less than 2 (Figure 31). For 8-PAM, with performance reaching an error floor for a BER of 10^{-5}, the Falconer-DFE-MLSE receiver is unsuitable. The only receiver with nonlinear equalization that meets the specifications for limited complexity is the Falconer-MLSE.
In parallel with our work, in December 2024, a team published an article [7] providing a very comprehensive state-of-the-art review of equalization methods used in very high-speed serial links. They detail the concrete implementation of the systems from a circuit perspective and compare the proposed nonlinear equalization solutions in terms of BER, energy efficiency, computational complexity, and area occupied. The systems with the most interesting characteristics are those combining linear filtering, DFE, and MLSE based on the Viterbi algorithm [34], [35] and [36]. We converged on the same type of receiver, but we also found that the structure of the optimal receiver depended on several parameters (channel impulse response shape and modulation order). Our receiver with a linear filtering-DFE-MLSE structure differs from those proposed in the literature in terms of the linear filtering strategy used (phase correction followed by Falconer filter).

8. Conclusion

To conclude this chapter, we summarize the observations and conclusions made for each receiver considered in Table 1. To be suitable for very high-speed serial links, a receiver must

have limited computational complexity, a maximum FBF of two coefficients when a DFE is used to shorten the channel, and achieve a BER of 10^{-5} for an $E_b/N_0 = 30$dB ratio.

Table 1 Summary table of the advantages and disadvantages of the different receivers studied. Receivers whose names are in green are those likely to meet the standard's specifications.

Receiver	Advantages	Disadvantages
DFE alone	Limited complexity and thermal noise amplification	Error propagation
MLSE alone	Optimal performance	High complexity
Linear filtering alone	Limited complexity, space requirements, and power consumption	Thermal noise amplification
Falconer-MLSE	Limited complexity	Amplification of thermal noise
DFE-MLSE	Limited amplification of thermal noise and error propagation	FBF too long
MLDFE	Same as above	Complexity too high
Falconer-DFE-MLSE	Limited complexity	Thermal noise amplification and error propagation

For the channel under consideration, synchronous linear ZF filtering meets the specifications imposed by the standard, as shown by the performance illustrated in Figure 12. MLSE alone is too complex, and DFE alone has an FBF with more than two coefficients to verify the ZF criterion.

Of the first three nonlinear receivers considered, Falconer-MLSE, DFE-MLSE, and MLDFE, only Falconer-MLSE meets all three requirements. In fact, MLDFE is the most efficient receiver studied in terms of BER, but the execution time of the VA makes it incompatible with decision feedback equalization. The DFE-MLSE rivals the MLDFE in the scenario ($\nu + 1 = 4$, 4-PAM) and the scenario ($\nu + 1 = 5$, 8-PAM), but the FBF has more than two coefficients. The Falconer-MLSE, on the other hand, does not require decision feedback and can reduce the size of the channel impulse response to two coefficients.

In order for the DFE-MLSE to meet the FBF size criterion, the channel is first shortened using the Falconer filter. This new combination, called Falconer-DFE-MLSE, performs 2dB worse in the scenario ($\nu' + 1 = 3$, $\nu + 1 = 2$, 4-PAM) than the Falconer-MLSE and reaches an error floor for a BER of 10^{-5} in the scenario ($\nu' + 1 = 3$, $\nu + 1 = 2$, 8-PAM). We note that when we remove the constraint on the maximum number of FBF coefficients, Falconer-DFE-MLSE can perform better than Falconer-MLSE, as in the scenario ($\nu' + 1 = 4$, $\nu + 1 = 2$, 4-PAM), for example.

The three receivers we have therefore selected for equalizing very high-speed SerDes links are synchronous linear ZF filtering, Falconer-MLSE, and Falconer-DFE-MLSE. Their name is written in green in Table 1. Although the synchronous ZF filter has the lowest computational complexity, in cases where the channel spectrum has one or more zeros (very strong attenuation), linear filtering alone cannot adequately equalize the channel , justifying the use of VA. Furthermore, Falconer-DFE-MLSE remains interesting when more degrees of freedom are granted to the system, which is conceivable with future technological advances. The three receivers can therefore be considered according to the channel and the modulation order.

Bibliography

[1] C. A. Belfiore and J. H. Park, “Decision feedback equalization,” Proceedings of the IEEE, vol. 67, no. 8, pp. 1143–1156, 1979.
[2] A. Viterbi, “Error bounds for convolutional codes and an asymptotically optimum decoding algorithm,” IEEE transactions on Information Theory, vol. 13, no. 2, pp. 260–269, 1967.
[3] A. Viterbi, “Convolutional codes and their performance in communication systems,” IEEE Transactions on Communication Technology, vol. 19, no. 5, pp. 751–772, 1971.
[4] G.D. Forney, “Maximum-likelihood sequence estimation of digital sequences in the presence of intersymbol interference,” IEEE Trans. Inf. Theory, 18(3): 363–378, 1972.
[5] J. K. Omura, “Optimal receiver design for convolutional codes and channels with memory via control theoretical concepts,” Information Sciences, vol. 3, no. 3, pp. 243–266, 1971.
[6] H. Kobayashi, “Application of probabilistic decoding to digital magnetic recording systems,” IBM Journal of Research and Development, vol. 15, no. 1, pp. 64–74, 1971.
[7] S. Jang, J. Lee, Y. Choi, D. Kim, and G. Kim, “Recent advances in ultra-high-speed wireline receivers with adc-dsp-based equalizers,” IEEE Open Journal of the Solid-State Circuits Society, 2024.
[8] R. Mellitz, “A collection of Cabled Backplane Prototype Channels for 200 Gbps per lane for .3df PHY type development” IEEE P802.3df & IEEE P802.3dj Tools and Channel Data Area, slide 11:
https://www.ieee802.org/3/df/public/adhoc/electrical/22_0502/mellitz_3df_elec_01_220502.pdf
[9] H. Kobayashi, “Correlative level coding and maximum-likelihood decoding,” IEEE Transactions on Information Theory, vol. 17, no. 5, pp. 586–594, 1971.
[10] F. Magee and J. Proakis, “Adaptive maximum-likelihood sequence estimation for digital signaling in the presence of intersymbol interference (corresp.),” IEEE Transactions on Information Theory, vol. 19, no. 1, pp. 120–124, 1973.
[11] S. Qureshi and E. Newhall, “Adaptive receiver for data transmission over time-dispersive channels,” IEEE Transactions on Information Theory, vol. 19, no. 4, pp. 448–457, 1973.
[12] G. D. Forney, “The viterbi algorithm,” Proceedings of the IEEE, vol. 61, no. 3, pp. 268–278, 1973.
[13] T. Ericson, “Structure of optimum receiving filters in data transmission systems (corresp.),” IEEE Transactions on Information Theory, vol. 17, no. 3, pp. 352–353, 1971.
[14] J.-M. Brossier, Signal et communication numérique : égalisation et synchronisation. Hermés science, 1997.

[15] R. W. Lucky, “Automatic equalization for digital communication,” Bell System Technical Journal, vol. 44, no. 4, pp. 547–588, 1965.
[16] T. Klein and J. Wolf, “On the use of channel introduced redundancy for error correction,” IEEE Transactions on Communication Technology, vol. 19, no. 4, pp. 396–402, 1971.
[17] D. D. Falconer and F. Magee Jr, “Adaptive channel memory truncation for maximum likelihood sequence estimation,” Bell Syst. Tech., 52(9): 1541–1562, 1973.
[18] N. Al-Dhahir and J. M. Cioffi, “Efficiently computed reduced-parameter input-aided mmse equalizers for ml detection : A unified approach,” IEEE Transactions on Information Theory, vol. 42, no. 3, pp. 903-915, 1996.
[19] C. Beare, “The choice of the desired impulse response in combined linear-viterbi algorithm equalizers,” IEEE Trans. Comm., 26(8): 1301–1307, 1978.
[20] D. G. Messerschmitt, “A geometric theory of intersymbol interference : Part i : Zero-forcing and decision-feedback equalization,” Bell System Technical Journal, vol. 52, no. 9, pp. 1483–1519, 1973.
[21] M. E. Austin, “Decision-feedback equalization for digital communication over dispersive channels.,” 1967.
[22] P. Monsen, “Feedback equalization for fading dispersive channels,” IEEE Transactions on Information Theory, vol. 17, no. 1, pp. 56–64, 1971.
[23] W. Lee and F. Hill, “A maximum-likelihood sequence estimator with decision-feedback equalization,” IEEE Transactions on Communications, vol. 25, no. 9, pp. 971–979, 1977.
[24] J. Labat, O. Macchi, and C. Laot, “Adaptive decision feedback equalization : Can you skip the training period ?,” IEEE Transactions on Communications, vol. 46, no. 7, pp. 921–930, 2002.
[25] R. Price, “Nonlinearly feedback-equalized pam vs. capacity,” in Proc. IEEE International Conferences on Communications, Philadephia, Penn, 1972.
[26] J. Salz, “Optimum mean-square decision feedback equalization,” Bell System Technical Journal, vol. 52, no. 8, pp. 1341–1373, 1973.
[27] E. Shamash and K. Yao, “On the structure and performance of a linear decision feedback equalizer based on the minimum error probability criterion,” in International Conference on Communications, 10 th, Minneapolis, Minn, p. 25, 1974.
[28] J. M. Cioffi, G. P. Dudevoir, M. V. Eyuboglu, and G. D. Forney, “Mmse decision-feedback equalizers and coding. i. equalization results,” IEEE transactions on Communications, vol. 43, no. 10, pp. 2582–2594, 1995.
[29] M. E. Meybodi, H. Gomez, Y.-C. Lu, H. Shakiba, and A. Sheikholeslami, “Design and implementation of an on-demand maximum-likelihood sequence estimation (mlse),” IEEE Open Journal of Circuits and Systems, vol. 3, pp. 97–108, 2022.
[30] M.-A. LaCroix, H. Wong, Y. H. Liu, H. Ho, S. Lebedev, P. Krotnev, D. A. Nicolescu, D. Petrov, C. Carvalho, S. Alie, et al., “6.2 a 60gb/s pam-4 adc-dsp transceiver in 7nm cmos with snr-based adaptive power scaling achieving 6.9 pj/b at 32db loss,” in 2019 IEEE International Solid-State Circuits Conference-(ISSCC), pp. 114–116, IEEE, 2019.
[31] J. Bailey, H. Shakiba, E. Nir, G. Marderfeld, P. Krotnev, M.-A. LaCroix, D. Cassan, and D. Tonietto, “A 112-gb/s pam-4 low-power nine-tap sliding-block dfe in a 7-nm finfet wireline receiver,” IEEE Journal of Solid-State Circuits, vol. 57, no. 1, pp. 32–43, 2021.
[32] D. Kim, Y. Choi, J. Lee, S. Jang, S. Song, M. Braendli, T. Morf, M. Kossel, P.-A. Francese, and G. Kim, “A loop-break decision feedback equalizer for dac/adc-dsp-based wireline transceivers,” IEEE Transactions on Circuits and Systems I : Regular Papers, 2024.

[33] Y. Gu and T. Le-Ngoc, "Adaptive combined dfe/mlse techniques for isi channels," IEEE Transactions on communications, vol. 44, no. 7, pp. 847–857, 1996.
[34] D. Pfaff, M. Nummer, N. Hai, P. Xia, K. G. Yang, M.-M. Mohsenpour, M.-A. LaCroix, B. Zamanlooy, T. Eeckelaert, D. Petrov, et al., "7.3 a 224gb/s 3pj/b 40db insertion loss transceiver in 3nm finfet cmos," in 2024 IEEE International Solid-State Circuits Conference (ISSCC), vol. 67, pp. 128–130, IEEE, 2024.
[35] S. Song, K. D. Choo, T. Chen, S. Jang, M. P. Flynn, and Z. Zhang, "A maximum-likelihood sequence detection powered adc-based serial link," IEEE Transactions on Circuits and Systems I : Regular Papers, vol. 65, no. 7, pp. 2269–2278, 2017.
[36] H. Yueksel, M. Braendli, A. Burg, G. Cherubini, R. D. Cideciyan, P. A. Francese, S. Furrer, M. Kossel, L. Kull, D. Luu, et al., "Design techniques for high-speed multi-level viterbi detectors and trellis-coded-modulation decoders," IEEE Transactions on Circuits and Systems I : Regular Papers, vol. 65, no. 10, pp. 3529–3542, 2018.
[37] Miqueu, P., Belveze, F., Brossier, J. M., & Ros, L. "Non-linear equalization techniques for high data rates serial links." ARCI'2025 international conference, Automation, Robotics & Communications for Industry 4.0/5.0, p. 154, February 2025.
[38] Miqueu, P., Belveze, F., Brossier, J. M., & Ros, L. "Parameters setting based on bit error probability formula for an amplitude modulated, baseband, communication system affected by timing jitter and frequency selective channel". *AEU-International Journal of Electronics and Communications*, *178*, 155288. 2024
[39] IEEE P802.3df & IEEE P802.3dj Tools and Channel Data Area, https://www.ieee802.org/3/df/public/tools/index.html
[40] IEEE P802.3df 200 Gb/s, 400 Gb/s, 800 Gb/s, and 1.6 Tb/s Ethernet Task Force Architecture and Logic Ad Hoc Area, slide 5: https://www.ieee802.org/3/df/public/adhoc/logic/22_0411/wang_3df_logic_220411.pdf